

Electronic and magnetic properties of hexagonal rare-earth-Zn-Mg compounds and their relation to the properties of icosahedral alloys

This article has been downloaded from IOPscience. Please scroll down to see the full text article.

2000 J. Phys.: Condens. Matter 12 5831

(<http://iopscience.iop.org/0953-8984/12/27/302>)

View [the table of contents for this issue](#), or go to the [journal homepage](#) for more

Download details:

IP Address: 171.66.16.221

The article was downloaded on 16/05/2010 at 05:18

Please note that [terms and conditions apply](#).

Electronic and magnetic properties of hexagonal rare-earth–Zn–Mg compounds and their relation to the properties of icosahedral alloys

M Krajčů†‡ and J Hafner†

† Institut für Material Physik and Centre for Computational Materials Science, Universität Wien, Sensengasse 8/12, A-1090 Wien, Austria

‡ Institute of Physics, Slovak Academy of Sciences, Dúbravská Cesta 9, SK-84228 Bratislava, Slovak Republic

Received 24 January 2000

Abstract. The electronic and magnetic structure of hexagonal rare-earth–zinc–magnesium compounds closely related to the icosahedral phases has been investigated by local density approximation (LDA) and LDA + U calculations. It is shown that both non-magnetic Y–Zn–Mg and antiferromagnetic Gd–Zn–Mg are stabilized by a Hume-Rothery-like electronic mechanism, the formation of a deep structure-induced pseudogap at the Fermi level being effected by an intra-atomic $s \rightarrow d$ promotion of the rare-earth sites and a strong s, p – d hybridization. The antiferromagnetism of Gd–Zn–Mg is of a layered type; the exchange coupling is an indirect Ruderman–Kittel–Kasuya–Yosida (RKKY) interaction between the localized 4f moments via the delocalized conduction electrons. The significance of the present results for the electronic and magnetic properties of the icosahedral alloys is discussed.

1. Introduction

The discovery of a new family of thermodynamically stable icosahedral phases in the RE–Zn–Mg (RE = Y, Gd, Tb, Dy, Ho or Er) systems [1, 2] has generated enormous interest because of the opportunity afforded to investigate the influence of quasiperiodicity on the magnetism of localized 4f electrons. Previous investigations of magnetism in quasicrystalline alloys reported diamagnetism, paramagnetism, ferromagnetism and spin-glass behaviour depending on structure, composition and thermal treatment (see, e.g., the references collected by Hafner and Krajčů [3, 4] and the recent review by Fukamichi [5]). One of the most striking results is the existence of two classes of transition-metal sites in ferromagnetic, paramagnetic and spin-glass systems differing strongly in their magnetic character. In icosahedral and decagonal Al–Pd–Mn alloys only a small fraction of the Mn atoms carry relatively large magnetic moments, suggesting that eventually magnetism is incompatible with the long-range quasiperiodic order and that the observed large local moments are to be attributed to defects in the quasicrystalline lattice. This view seems to be supported by the similarity of the magnetic properties of quasicrystalline and amorphous alloys [6] and by the observation of a dramatic increase of the paramagnetic susceptibility on the melting of quasicrystalline alloys [7]. Detailed investigations of the conditions for the formation of magnetic moments in icosahedral and decagonal Al–Pd–Mn alloys using local spin-density-functional techniques [3, 4] have demonstrated that a strong Al p –Mn d hybridization does indeed suppress magnetism in all related crystalline phases and at most sites of the quasicrystalline lattices. The sites carrying

magnetic moments are characterized by enhanced Mn–Mn coordination and looser-than-average Al–Mn coordination, allowing the local Mn electronic density of states (DOS) to fulfil the Stoner criterion for the formation of an itinerant magnetic moment.

For icosahedral $\text{RE}_8\text{Zn}_{50}\text{Mg}_{42}$ (RE = Gd, Tb, Dy) a Curie–Weiss-type temperature dependence of the dc magnetic susceptibility with effective magnetic moments close to that of free RE^{2+} ions and a negative value of the paramagnetic Curie temperature has been reported [8, 9], suggesting that the RE–RE exchange interaction is antiferromagnetic. The magnetic cooling effect observed in the magnetic susceptibility suggests that the RE–Zn–Mg quasicrystals are spin-glass systems with spin-freezing temperatures of $T_f = 7.6$ K (RE = Tb) and $T_f = 5.5$ K (RE = Gd). On the basis of magnetic powder neutron diffraction measurements, Charrier *et al* [10] claimed evidence for a quasiperiodic type of antiferromagnetic (AFM) long-range order at $T_N > T_f$ for RE = Tb, Ho, Dy and Er. However, the intensity of the sharp magnetic Bragg peaks indicative of antiferromagnetic ordering is small and superposed by considerable diffuse scattering. This claim was contested by Islam *et al* [11] who demonstrated that no evidence for AFM ordering exists for samples prepared from slowly solidified large single-grain specimens whereas some magnetic superstructure peaks can be found for rapidly quenched alloys. Hence it was suggested that the additional diffraction peaks should be attributed to antiferromagnetic ordering not in the quasicrystal, but in a RE-containing second, possibly crystalline phase. Evidence for the coexistence of a closely related crystalline RE–Zn–Mg phase was indeed found by Fisher *et al* [12] for $\text{Tb}_7\text{Zn}_{62}\text{Mg}_{31}$ and by Sato *et al* [13] for $\text{Ho}_{16}\text{Zn}_{68}\text{Mg}_{16}$. So far, all results discussed here refer to face-centred icosahedral RE–Zn–Mg quasicrystals. For simple icosahedral $\text{Gd}_x\text{Zn}_{70-x}\text{Mg}_{30}$ quasicrystals, Sato *et al* [13] have reported that negative values of the effective paramagnetic Curie temperature increase with increasing Gd content, indicating an increasing strength of antiferromagnetic exchange coupling.

The icosahedral RE–Zn–Mg alloys also exhibit other outstanding electronic properties. For non-magnetic Y–Zn–Mg quasicrystals the measured electronic specific heat suggests the existence of a pseudogap in the electronic DOS at the Fermi level ($\gamma_{\text{exp}}/\gamma_{\text{free-el}} \approx 0.7$, where γ is the coefficient of the linear term in the temperature-dependent specific heat) [14]. Similar pseudogaps have been reported for the free-electron-like quasicrystals Al–Zn–Mg and Al–Cu–Li [15–17] and explained in terms of a generalized Hume–Rothery mechanism. Since all RE elements forming an icosahedral phase are trivalent and the RE content varies only in a rather narrow interval, their electron/atom ratio is almost constant, $e/A \approx 2.06$ – 2.09 . In icosahedral Gd–Zn–Mg the magnetic contribution to the specific heat exhibits a broad maximum just above the spin-freezing temperature similar to that observed in quasicrystalline Al–Pd–Mn and in conventional spin-glass systems [14]. From the values of magnetic entropy near T_f it has been argued that the observed spin-glass behaviour is due to fluctuating RKKY exchange interactions rather than to random anisotropies like in many crystalline RE alloys [18]. Electronic and thermal conductivity data agree with the existence of a pseudogap in the electronic DOS: the resistivity is comparable to that in other s, p-bonded quasicrystals; the temperature coefficient is negative [8, 19].

2. Structure

Despite of the fact that the RE–Zn–Mg quasicrystals belong to the best-ordered quasicrystalline phases, no generally accepted atomic model for their structure has emerged. On the basis of HRTEM studies it was proposed that the RE atoms preferentially occupy sites at the centre of icosahedra and are surrounded by Zn and Mg [20]. Kounis *et al* [21] reported that the structure of $i\text{-RE}_x\text{Zn}_{60}\text{Mg}_{40-x}$ is simple icosahedral (i) for $x < 7$ and face-centred icosahedral for

$x > 7$. In the latter case, the projection of a rhombic triacontahedron was found in HRTEM images taken along a twofold axis. Very recently Abe *et al* [22] reported the existence of a decagonal (d) phase in the Dy–Zn–Mg system with a structure similar to that of the high-temperature phase of crystalline Zn_7Mg_4 in which the atoms form a planar pentagonal network. The structure of d-Dy–Zn–Mg was described as a Penrose tiling decorated by individual atoms. This contrasts with the generally accepted models for most icosahedral and decagonal phases based on decorations with large non-crystallographic clusters. For stoichiometries close to the i-RE–Zn–Mg phases, Abe *et al* reported the existence of three distinct hexagonal phases. The hexagonal crystals transform reversibly into the high-temperature icosahedral phase, suggesting a close structural relationship between the hexagonal and icosahedral phases.

Hexagonal phases in the Y–Zn–Mg and Sm–Zn–Mg systems were resolved by Takakura *et al* [23] and Singh *et al* [24] and found to be isostructural with the Sm–Zn–Mg structure described previously by Drits *et al* [25]. The structure of hexagonal Y–Zn–Mg is closely related to that of the hexagonal Laves phase $MgZn_2$ whose basic constituents are intrapenetrating icosahedra (formed by six Mg and six Zn and centred on Zn) and Friauf polyhedra (twelve vertices being occupied by Zn and four by Mg with a Mg atom at the centre). In the Laves phase, Friauf polyhedra and icosahedra form a dense three-dimensional network. Alternatively, the Laves phase may be described as a stacking of Kagomé layers (Zn), hexagonal layers (Mg) and triangular (Zn) layers [26]. In hexagonal RE–Zn–Mg, groups of triangles of Zn atoms are each replaced by a single Y atom such that large Y triangles with an edge length of 5.53 Å are formed (see figure 1). If the Y environment is similar in the icosahedral phase, this contradicts the icosahedral site symmetry claimed on the basis of the HRTEM. In the hexagonal layers the Mg atoms lying above or below Y atoms are replaced by Zn, while the triangular layers remain occupied by Zn only. All layers are slightly distorted. As a result of these changes, the three-dimensional network of Friauf polyhedra interconnected by icosahedra is replaced by a columnar structure. Each column is made up of three Friauf polyhedra in each layer, stacked along the hexagonal axis. Different columns are linked at the level of the Kagomé net by Y atoms, and by Zn atoms at the level of the hexagonal and triangular layers.

The structural relationship between the hexagonal phase and the icosahedral phase has been discussed by Singh *et al* [24], suggesting that the relation between the hexagonal and the icosahedral phase is similar to that between an icosahedral and a decagonal phase: the sixfold axis of the crystalline structure corresponding to a twofold axis of the quasicrystal. Takakura *et al* [23] have pointed out that the Zn atoms located at the cores of the columnar clusters are located at the centres of interpenetrating icosahedra, and identified pseudo-fivefold axes common to pairs of tetrahedra. However, a complete atomically resolved structural model for the icosahedral phase is not available to date.

The important point is that icosahedral RE–Zn–Mg alloys do not belong to the two most important classes of icosahedral structures (Al–transition-metal quasicrystals based on large clusters of the type of Macay icosahedra and Al–s, p metal quasicrystals of Frank–Kasper type forming Bergman clusters), but form a different type of local atomic arrangement.

The present paper is devoted to investigation of the electronic structure of hexagonal Y–Zn–Mg and Gd–Zn–Mg and to a discussion of the magnetic ordering in the Gd-based alloys, with special attention paid to the significance of these results for the possible magnetic ordering in icosahedral RE–Zn–Mg.

3. Methodology—LSDA versus LDA + U

Modern electronic structure calculations for magnetic materials are based on the local spin-density approximation (LSDA). The LSDA has been widely applied to atoms and molecules.

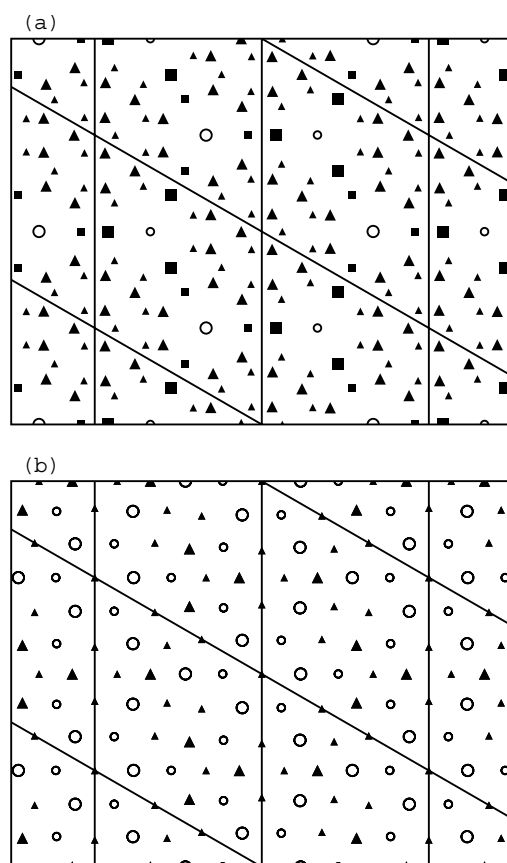


Figure 1. Atomic layers building the structure of hexagonal Y–Zn–Mg. (a) The planar layer at $z = 0.25$ is represented by larger symbols; the planar layer at $z = 0.75$ related to that at $z = 0.25$ by mirror symmetry is represented by smaller symbols. The triangles represent Zn atoms, the squares Y atoms. Note how the Kagomé network of the Zn atoms is disrupted by Y atoms, each replacing a triangle of Zn atoms. (b) The puckered layer located between $z \approx 0.39$ and $z \approx 0.61$. Triangles and circles represent Zn and Mg atoms, respectively. Here the honeycomb network of Mg atoms appearing in MgZn_2 is broken by a Mg/Zn substitution in the region between the columns formed by Friauf polyhedra. See the text.

While it is quite successful in finding the ground state for a variety of materials, some failures are also known. In the present context, the most notable failures of the LSDA are that of not predicting the correct magnetic ground state for metals such as Fe, Mn or Gd and that of seriously underestimating the exchange splitting in magnetic materials with narrow d or f bands. While it has been demonstrated that the former problem can be solved by introduction gradient corrections to the exchange–correlation functional (see Moroni *et al* [27] for Fe, Asada and Terakura [28] and Eder *et al* [29] for Mn), the problem is more complex for RE elements such as Gd. While the work of Heinemann and Temmerman [30] has demonstrated that generalized gradient corrections also stabilize the ferromagnetic state over the antiferromagnetic order preferred in the LSDA, the LSDA is definitely insufficient to predict the correct positions of the occupied and empty f bands relative to the Fermi level, due to the failure to account for the strong electron–electron interaction in the narrow f bands. Attempts to improve on the LSDA in this respect have been based on self-interaction corrections (SIC) [31] and on the

so-called LDA + U approximation [32]. The SIC approach reproduces quite well the localized nature of the 4f orbitals and accounts for the variation of the valency with the progressive filling of the band [33], but SIC one-electron energies are in disagreement with spectroscopic data. In the LDA + U approach the valence electrons are separated into two subsystems: localized f or d electrons for which the Coulomb interaction is taken into account as in a mean-field approximation by a term $\frac{1}{2} \sum_{i \neq j} n_i n_j$ (where the n_i stand for orbital occupancies) and delocalized electrons described by the LDA [32, 34]. Subtracting the total Coulomb energy of the localized electrons given by $UN(N - 1)/2$, with $N = \sum_i n_i$, from the LSDA energy and adding this Hubbard-like term leads to the LDA + U functional (neglecting here for simplicity exchange and correlation):

$$E = E_{LDA} - UN(N - 1)/2 + \frac{1}{2} \sum_{i \neq j} n_i n_j. \quad (1)$$

The orbital energies ϵ_i are given by the derivatives of the total energy with respect to the orbital occupancies n_i :

$$\epsilon_i = \frac{\partial E}{\partial n_i} = \epsilon_{i,LDA} + U \left(\frac{1}{2} - n_i \right). \quad (2)$$

Hence the orbital energies for occupied and empty states are shifted by $\pm U/2$. For a more detailed description of the LDA + U method and for a calculation of the electron–electron interaction terms based on atomic orbitals, we refer the reader to the reviews by Anisimov *et al* [34, 35].

For Gd a calculation based on the localized 4f orbitals of the Gd^{3+} ion in the $^8\text{S}_{7/2}$ ground state yields screened Coulomb and exchange parameters of $U = 6.7$ eV and $J = 0.7$ eV. Hence the separation between occupied and empty f states given by $U + 6J$ is ≈ 11 eV and in good agreement with the experimental value of ≈ 12 eV derived from photoemission and inverse photoemission spectroscopies [36]. In the LSDA calculation the exchange splitting is very seriously underestimated. In our calculations for icosahedral Gd–Zn–Mg we have used the same parameters for the LDA + U Hamiltonian.

LDA + U calculations are straightforwardly implemented in techniques using atomic-orbital-type basis sets. In the present case we use the linear muffin-tin orbital method in the atomic-sphere approximation (LMTO-ASA) [37, 38]. For Y–Zn–Mg the LDA has been used and for Gd–Zn–Mg the LDA + U has been used.

4. Results

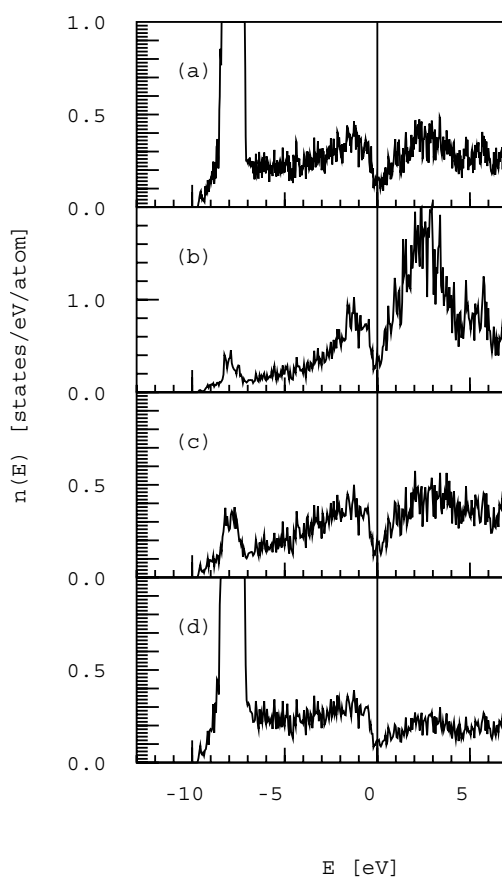
4.1. Nonmagnetic Y–Zn–Mg

We begin by discussing the electronic structure of non-magnetic $\text{Y}_{6.52}\text{Zn}_{65.22}\text{Mg}_{28.26}$ calculated for the structure determined by Takakura *et al* [23]. The atomic coordinates are listed in table 1. Site 8, for which a fractional occupancy of $\text{Mg}/\text{Y} = 0.842/0.158$ has been determined experimentally, has been occupied by Mg atoms only, resulting in a slightly reduced overall Y content. The electronic spectrum calculated for a set of 133 k -points in the irreducible part of the Brillouin zone is shown in figure 2. The total density of states shows a broad free-electron-like band (with occupied bandwidth ≈ 9.7 eV) overlapping at its bottom with a narrow Zn d band (width about 1.5 eV) and near the Fermi level with the lower part of a very broad Y d band. The most significant feature, however, is the very deep DOS minimum centred exactly at the Fermi level.

Figure 3 shows the powder diffractogram calculated for hexagonal Y–Zn–Mg. We find that the diameter $2k_F = 3.04 \text{ \AA}^{-1}$ of the free-electron Fermi sphere falls at the centre

Table 1. Atomic coordinates in hexagonal Y–Zn–Mg (space group $P6_3/mmc$, lattice constants $a = 14.62 \text{ \AA}$, $c = 8.78 \text{ \AA}$).

Atom	Site	x	y	z
Zn1	12j	0.409670	0.291200	0.250000
Zn2	12i	0.359800	0.000000	0.000000
Zn3	12j	0.240630	0.305090	0.250000
Zn4	12k	-0.432890	0.134220	0.415540
Zn5	6h	0.061530	0.123060	0.250000
Zn6	4f	0.333333	-0.333333	0.101900
Zn7	2a	0.000000	0.000000	0.000000
Mg1	2d	0.333333	-0.333333	-0.250000
Mg2	12k	-0.228700	-0.457400	-0.447200
Mg3	12k	0.116600	0.233200	-0.435500
Y	6h	0.458840	-0.082319	0.250000

**Figure 2.** The electronic density of states (DOS) of hexagonal $Y_{6.5}Zn_{65.2}Mg_{28.3}$. (a) The total DOS; (b) the partial Y DOS, (c) partial Mg DOS and (d) partial Zn DOS.

of several intense, narrowly spaced diffraction peaks for the hexagonal structure. These peaks are nearly coincident with the (222100) Bragg peak of the icosahedral phase; see figure 3. Hence the pseudogap is indeed structure induced. Pseudogaps at the Fermi level

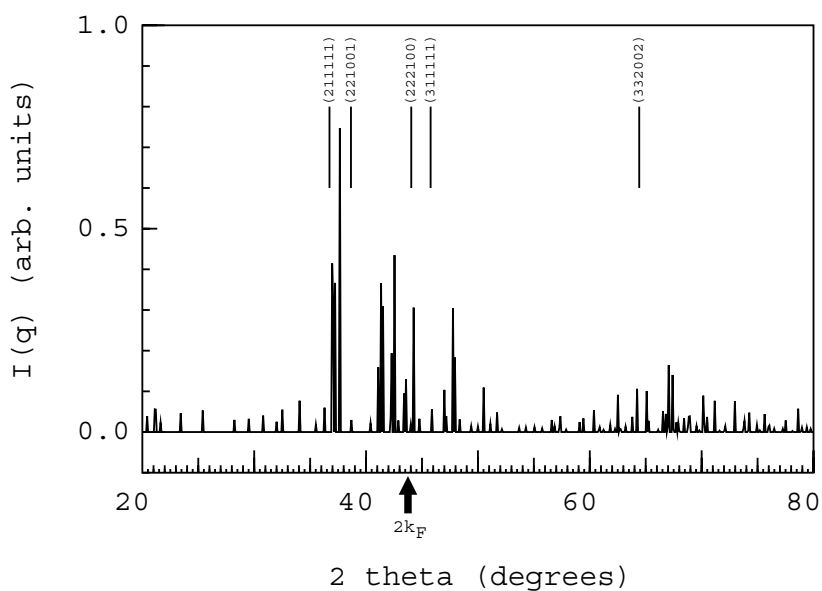


Figure 3. The powder diffractogram calculated for hexagonal Y–Zn–Mg. The diameter $2k_F = 3.04 \text{ \AA}^{-1}$ of the free-electron Fermi sphere falls at the centre of several intense, narrowly spaced diffraction peaks (arrow). Vertical line segments indicate the positions of some prominent peaks for icosahedral Y–Zn–Mg.

have been also reported both from theory and experiment for the Laves phase MgZn_2 and for all rational approximants of icosahedral Al–Zn–Mg (the lowest approximant being the Frank–Kasper phase $\text{Al}_{13}\text{Mg}_{32}\text{Zn}_{30}$) [16]. For the Frank–Kasper phase Al–Zn–Mg (and for all higher approximants to the icosahedral phase), the calculated DOS at the Fermi level is $n(E_F) \approx 0.17$ states $\text{eV}^{-1}/\text{atom}$ (to be compared with a free-electron DOS of $n(E_F) \approx 0.36$ states $\text{eV}^{-1}/\text{atom}$), while the experimentally measured DOSs range between $n(E_F) = 0.30$ and 0.33 states $\text{eV}^{-1}/\text{atom}$. The difference is to be attributed to the substantial degree of Al/Zn substitutional disorder and phason disorder present in icosahedral Al–Zn–Mg. For the hexagonal C14-type Laves phase MgZn_2 , the electronic spectrum is rather similar to that reported here for hexagonal Y–Zn–Mg [39]. Due to the less complex crystal structure (6 atoms/cell), the Laves phase is strongly structured by Van Hove singularities—in contrast to the very spiky DOS of Y–Zn–Mg. However, altogether the DOS of the Laves phase fluctuates around the Fermi level and a Hume-Rothery-like mechanism does not seem to play a decisive role in determining phase stability. This is also confirmed by a detailed theoretical [39] and experimental [41] analysis of the differential charge densities.

The more pronounced pseudogap in hexagonal Y–Zn–Mg compared to the Al–Zn–Mg Frank–Kasper phase and to the MgZn_2 Laves phase is due to a strong s, p–d hybridization arising from the presence of Y. This is demonstrated by the angular-momentum-decomposed Y DOS shown in figure 4. For Zn and Mg, the DOS at the Fermi level is predominantly p-like, as in the Frank–Kasper and Laves phases. At the Y sites the electronic DOS has a very strong d character with only a weak p and s admixture. The intra-atomic $s \rightarrow d$ promotion at Y sites is the consequence of a locally increased electronic pressure arising from a very dense local coordination: Y has 18 nearest neighbours (14 Zn and 4 Mg) at distances ranging from 3.01 \AA to 3.43 \AA (for details, see table 2). Y interacts rather strongly with the Zn atoms: of the seven inequivalent Zn sites, five have between one and three Y neighbours; only the two sites

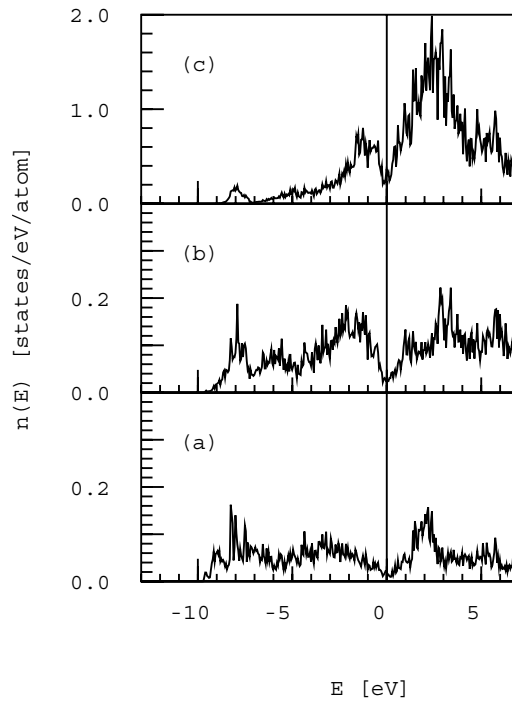


Figure 4. The angular-momentum-decomposed local DOS at the Y sites in hexagonal $Y_{6.5}Zn_{65.2}Mg_{28.3}$. Panels (a) to (c) show the s-, p- and d-electron DOSs, respectively.

Table 2. Coordination in hexagonal Y–Zn–Mg: the number of nearest neighbours (NN) and the corresponding distances in Å.

Atom	Zn–NN	Distances	Mg–NN	Distances	Y–NN	Distances
Zn1	6	2.53–2.66	5	3.01–3.49	1	3.35
Zn2	6	2.66–2.76	4	2.94–3.13	2	3.18
Zn3	5	2.58–2.66	6	2.89–3.18	1	3.33
Zn4	7	2.63–3.71	3	2.86–2.91	2	3.01–3.10
Zn5	6	2.64–2.70	6	3.03–3.09	0	
Zn6	4	2.60–3.01	4	3.03–3.09	3	3.43
Zn7	6	2.69	6	3.01	0	
Mg1	14	2.91–3.49	6	3.75	0	
Mg2	9	2.68–3.01	3	3.02–3.75	2	3.42
Mg3	12	3.01–3.18	4	3.02–3.26	0	
Y	14	3.01–3.43	4	3.42	0	

located in the columns formed by icosahedra and Friauf polyhedra have no Y neighbours. The Y–Mg interaction is weaker; only one of the three inequivalent Mg sites has two Y neighbours. Altogether we can conclude that in analogy to the Frank–Kasper phase Al–Zn–Mg, Y–Zn–Mg can be considered as a Hume-Rothery compound stabilized by a Brillouin-zone–Fermi-sphere interaction, with a pseudogap that is enhanced by s, p–d hybridization. The existence of a pronounced pseudogap in the electronic density of states agrees very well with the result of electronic specific heat measurements suggesting that the DOS at the Fermi level is reduced to about 70% of its free-electron value [14].

4.2. Antiferromagnetic Gd–Zn–Mg

As an example of the RE–Zn–Mg compounds with possible magnetic order we have selected Gd–Zn–Mg, because for the half-filled f band of Gd the magnetic order and exchange splitting are rather well described by a LDA + U approach [32, 34].

A conventional LSDA calculation produces a weakly spin-split Gd 4f band close to the Fermi level; the position and occupancy of the bands are very sensitive to even very small changes in the spin-dependent potential, so it is very difficult to achieve a converged result.

The LDA + U calculation has been performed using the Coulomb and exchange parameters determined by Anisimov *et al* [34, 36] for pure Gd: $U = 6.7$ eV, $J = 0.7$ eV. The calculation converges towards a layered antiferromagnetic order: Gd moments within the triangular Gd groups located in the planes at $z = 0.25$ and $z = 0.75$ couple ferromagnetically, but moments in neighbouring planes assume antiparallel orientations. This means that along the hexagonal axis we have a sequence of antiferromagnetically coupled layers with internal ferromagnetic ordering. The moments at the Gd sites are $\mu_{\text{Gd}} = \pm 7.32\mu_B$, i.e. almost equal to the moments in pure ferromagnetic Gd.

It is important to realize that the interatomic distances between Gd atoms in hexagonal Gd–Zn–Mg are much larger than in pure Gd: the distance between Gd atoms within the same triangle is about 5.44 Å; this is larger than the distance to the nearest Gd atom in the neighbouring layer which is only ≈ 4.9 Å. In pure hexagonal close-packed Gd, the nearest-neighbour distance is ≈ 3.37 Å. Hence in the Gd–Zn–Mg compound the exchange interaction switches from antiferromagnetic to ferromagnetic as the Gd–Gd distance increases from 4.9 Å to 5.4 Å, whereas the direct nearest-neighbour coupling in pure Gd is ferromagnetic around the equilibrium zero-pressure distance and becomes antiferromagnetic under compression [30]. This oscillatory variation suggests that in the Gd–Zn–Mg compound as well as in pure Gd, the dominant exchange interaction is promoted by an oscillatory RKKY-type coupling of the localized 4f electrons via the itinerant s, p, d electrons.

The spin-integrated total and local electronic densities of states are shown in figure 5. Except for the spin-split 4f bands of Gd located at -6.3 eV and $+5.2$ eV, the electronic spectrum is very similar to that calculated for Y–Zn–Mg; in particular we find a deep pseudogap at the Fermi level. The spin-polarized and angular-momentum-decomposed electronic densities of states at the Gd sites are shown in figure 6. The very narrow occupied 4f band is located in a region where the DOS at the Gd sites arises mostly from a resonance with the Zn 3d band. The narrowness of the 4f majority band reflects its very weak coupling to the s, p, d bands. The empty 4f band of Gd falls into a region of high 5d DOS; the band is broadened because of the more extended character of the empty 4f states and their stronger interaction with the d states. As in the Y compound, we find a strong interatomic s, p \rightarrow d transfer for the Gd states, contributing to the formation of a pseudogap at the Fermi level.

Hence our results lend credibility to the assertion that the antiferromagnetic polarization observed in icosahedral RE–Zn–Mg compounds [11] is indeed to be attributed to the presence of an antiferromagnetic crystalline phase. Our result that the exchange interactions are predominantly RKKY type agrees with conclusions drawn on the basis of investigations of the magnetic entropy [14, 18].

5. Discussion and conclusions

The main results of our study are as follows:

- (i) RE–Zn–Mg compounds are stabilized by a Hume-Rothery mechanism leading to the formation of a pseudogap in the electronic DOS at the Fermi level.

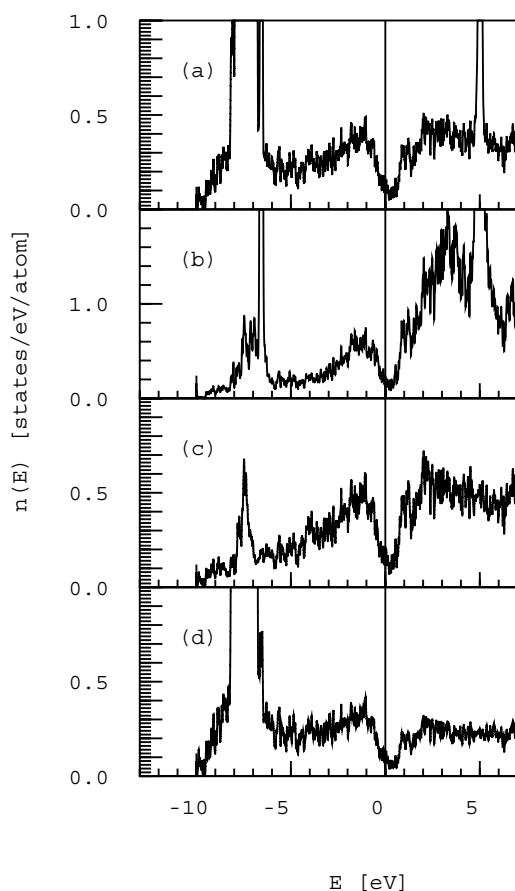


Figure 5. The electronic density of states (DOS) of hexagonal $\text{Gd}_{6.5}\text{Zn}_{65.2}\text{Mg}_{28.3}$. (a) The total DOS; (b) the partial Gd DOS, (c) partial Mg DOS and (d) partial Zn DOS.

- (ii) Compared to those for simple-metal Frank–Kasper phases (including Laves phases) based on Zn and Mg, the depth of the stabilizing pseudogap is enhanced by intra-electronic $s, p \rightarrow d$ promotion on the RE sites and a strong Zn–Mg s, p –RE d hybridization.
- (iii) Gd–Zn–Mg compounds (and presumably other icosahedral RE–Zn–Mg alloys containing f electrons) show layered antiferromagnetic ordering.
- (iv) RE exchange interactions are RKKY-like, i.e. indirect exchange interactions between the localized $4f$ electrons via the itinerant s, p, d electrons.

In the absence of a clear structural correlation between the hexagonal and icosahedral RE–Zn–Mg phases it is difficult to assess the significance of the present results for the quasicrystalline alloys. However, the fact that the hexagonal \longleftrightarrow icosahedral transition is reversible certainly represents an indication that many local arrangements are preserved during the transformation. Furthermore, the exceptional stability of the icosahedral alloys also suggests that they must receive a comparable degree of band-gap stabilization. Our result that the exchange interactions in the magnetic RE–Zn–Mg alloys are RKKY-like also lends credibility to suggestions that the icosahedral RE–Zn–Mg alloys show spin-glass behaviour: in the hexagonal Gd–Zn–Mg alloys, the layered antiferromagnetic order is determined by the fact that the exchange interaction changes sign between the first two Gd–Gd interatomic distances in and between the planes. Independently of details of the icosahedral structure, the Gd–Gd distances in the quasicrystalline phase will fluctuate around

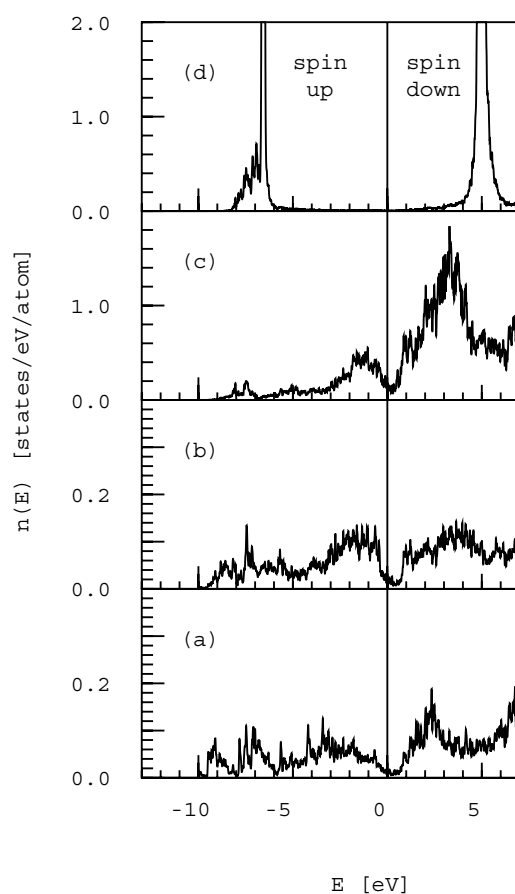


Figure 6. Spin-polarized and angular-momentum-decomposed local DOSs at the Gd sites in hexagonal $\text{Gd}_{6.5}\text{Zn}_{65.2}\text{Mg}_{28.3}$. Panels (a) to (d) show the s-, p-, d- and f-electron DOSs, respectively.

the dividing line between ferromagnetic and antiferromagnetic coupling, thus leading to spin-glass behaviour.

The situation is, however, quite different from the conditions leading to spin-glass behaviour in icosahedral Al–Pd–Mn. In i-Al–Pd–Mn the potentially magnetic Mn ions occur in a much higher concentration than the RE ions in i-RE–Zn–Mg. However, the conditions for formation of a magnetic Mn moment depend critically on the local environment and are satisfied only for a small number of magnetic ions located at large distances. In Gd–Zn–Mg on the other hand, all Gd ions carry localized moments, the mechanism of moment formation being completely intra-atomic. Gd ions interact over distances comparable to second- and third-neighbour distances in the pure metal via RKKY interactions showing an oscillatory distance dependence.

Acknowledgments

This work was supported by the Austrian Ministry for Research and Transport within the Project ‘Magnetism on the Nanometre Scale’ and through the Centre for Computational Materials Science. MK is also grateful for support from the Grant Agency for Science of Slovakia (No 2/6064/99).

References

- [1] Kuo Z, Zhang S, Tang Y and Zhan D 1993 *Scr. Metall. Mater.* **28** 1513
- [2] Tsai A P, Niikura A, Inoue A, Masumoto T, Nishida Y, Tsuda K and Tanaka M 1994 *Phil. Mag. Lett.* **70** 169
- [3] Hafner J and Krajčí M 1998 *Phys. Rev. B* **57** 2849
- [4] Krajčí M and Hafner J 1998 *Phys. Rev. B* **58** 14 110
- [5] Fukamichi K 1999 *Physical Properties of Quasicrystals* ed Z M Stadnik (Berlin: Springer) p 296
- [6] Godinho M, Berger C, Lasjaunias J C, Kasselbach K and Berthoux O 1990 *J. Non-Cryst. Solids* **117+118** 808
- [7] Hippert F, Audier M, Klein H, Bellissent R and Boursier D 1996 *Phys. Rev. Lett.* **76** 54
- [8] Hattori Y, Niikura A, Tsai A P, Inoue A, Masumoto T, Fukamichi K, Aruga-Katori H and Goto T 1995 *J. Phys.: Condens. Matter* **7** 2313
- [9] Charrier B and Smith D 1997 *J. Magn. Magn. Mater.* **171** 106
- [10] Charrier B, Ouladdiaf B and Smith D 1997 *Phys. Rev. Lett.* **78** 4637
- [11] Islam Z, Fisher I R, Zaretsky J, Canfield P C, Stassis C and Goldman A I 1998 *Phys. Rev. B* **57** R11 047
- [12] Fisher I R, Cheon K O, Panchula A F, Canfield P C, Chernikov M, Ott H R and Dennis K 1999 *Phys. Rev. B* **59** 308
- [13] Sato T J, Takakura H, Tsai A P and Shibato K 1998 *Phys. Rev. Lett.* **81** 2364
- [14] Hattori Y, Fukamichi K, Suzuki K, Niikura A, Tsai A P, Inoue A and Masumoto T 1995 *J. Phys.: Condens. Matter* **7** 4183
- [15] Hafner J and Krajčí M 1992 *Phys. Rev. Lett.* **68** 2321
- [16] Hafner J and Krajčí M 1993 *Phys. Rev. B* **47** 11 795
- [17] Hafner J and Krajčí M 1999 *Physical Properties of Quasicrystals* ed Z M Stadnik (Berlin: Springer) p 209
- [18] Hattori Y, Fukamichi K, Chikawa H, Aruga-Katori H and Goto T 1994 *J. Phys.: Condens. Matter* **6** 10 129
- [19] Gianno K, Fisher I R, Canfield P C and Ott H R 1999 *7th Int. Conf. on Quasicrystals (Stuttgart)* paper PD21
- [20] Kramer M J, Canfield P C, Fisher I R, Kycia S and Goldman A I 1999 *7th Int. Conf. on Quasicrystals (Stuttgart)* paper PB22
- [21] Kounis A, Micha G, Fuess H, Sterzel R and Assums W 1999 *7th Int. Conf. on Quasicrystals (Stuttgart)* paper PB21
- [22] Abe E, Sato T J, Takakura H and Tsai A P 1999 *7th Int. Conf. on Quasicrystals (Stuttgart)* paper OA3
- [23] Takakura H, Sato A, Yamamoto A and Tsai A P 1998 *Phil. Mag. Lett.* **78** 263
- [24] Singh A, Abe E and Tsai A P 1998 *Phil. Mag. Lett.* **77** 95
- [25] Drits M E, Rokhlin L L, Abrukina N P, Kinzhbalo V V and Tyvanchuk 1985 *Izv. Akad. Nauk SSSR, Met.* **6** 194
- [26] Pearson W B 1972 *The Crystal Chemistry and Physics of the Metals and Alloys* (New York: Wiley)
- [27] Moroni E G, Kresse G, Furthmüller J and Hafner J 1997 *Phys. Rev. B* **56** 15 629
- [28] Asada T and Terakura K 1993 *Phys. Rev. B* **47** 15 992
- [29] Eder H, Moroni E G and Hafner J 2000 *Phys. Rev. B* at press
- [30] Heinemann M and Temmerman W 1994 *Phys. Rev. B* **49** 4348
- [31] Svane A and Gunnarsson O 1990 *Phys. Rev. Lett.* **65** 1148
- [32] Anisimov V I, Zaanen J and Andersen O K 1991 *Phys. Rev. B* **44** 943
- [33] Strange P, Svane A, Temmerman W M, Szotek Z and Winter H 1999 *Nature* **399** 756
- [34] Anisimov V I, Aryasetiawan F and Lichtenstein A I 1997 *J. Phys.: Condens. Matter* **9** 767
- [35] Anisimov V I, Solovyev I V, Korotin M A, Czyzyk M T and Sawatzky G A 1993 *Phys. Rev. B* **48** 16 929
- [36] Harmon B N, Antropov V P, Lichtenstein A I, Solovyev J V and Anisimov V I 1995 *J. Phys. Chem. Solids* **56** 1521
- [37] Andersen O K 1975 *Phys. Rev. B* **12** 3060
- [38] Andersen O K, Jepsen O and Glötzel K 1985 *Highlights of Condensed Matter Theory* ed I Bassani, I Fumi and M P Tosi (Amsterdam: North-Holland)
- [39] Hafner J, Jaswal S S, Tegze M, Pflugi A, Krieg J, Oelhafen P and Güntherodt H J 1988 *J. Phys. F: Met. Phys.* **18** 2583
- [40] Hafner J 1985 *J. Phys. F: Met. Phys.* **15** 1879
- [41] Ohba T, Kitano Y and Komura Y 1984 *Acta Crystallogr. C* **40** 1